Dosimetry of [^{177}Lu]Lu-PSMA–Targeted Radiopharmaceutical Therapies in Patients with Prostate Cancer: A Comparative Systematic Review and Metaanalysis

Zachary Ells[1], Tristan R. Grogan[2], Johannes Czernin[1], Magnus Dahlbom*[1], and Jeremie Calais*[1]

[1]*Ahmanson Translational Theranostics Division, Department of Molecular and Medical Pharmacology, UCLA, Los Angeles, California; and* [2]*Department of Medicine Statistics Core, David Geffen School of Medicine, UCLA, Los Angeles, California*

Novel theranostic approaches using radiopharmaceuticals targeting prostate-specific membrane antigen (PSMA) have emerged for treating metastatic castration-resistant prostate cancer. The physical properties and commercial availability of ^{177}Lu make it one of the most used radionuclides for radiopharmaceutical therapy (RPT). In this literature review, we aimed at comparing the dosimetry of the most used [^{177}Lu]Lu-PSMA RPT compounds. **Methods:** This was a systematic review and metaanalysis of [^{177}Lu]Lu-PSMA RPT (617, I&T, and J591) dosimetry in patients with prostate cancer. Absorbed doses in Gy/GBq for each organ at risk (kidney, parotid and submandibular glands, bone marrow, liver, and lacrimal glands) and for tumor lesions (bone and nonbone lesions) were extracted from included articles. These were used to estimate the pooled average absorbed dose of each agent in Gy/GBq and in Gy/cycle, normalized to the injected activity (per cycle) used in the VISION (7.4 GBq), SPLASH (6.8 GBq), and PROSTACT trials (5.8 GBq). **Results:** Twenty-nine published articles comprising 535 patients were included in the metaanalysis. The pooled doses (weighted average across studies) of [^{177}Lu]Lu-PSMA-617 and [^{177}Lu]Lu-PSMA-I&T were 4.04 Gy/GBq (17 studies, 297 patients) and 4.70 Gy/GBq (10 studies, 153 patients) for the kidney ($P = 0.10$), 5.85 Gy/GBq (14 studies, 216 patients) and 2.62 Gy/GBq (5 studies, 86 patients) for the parotids ($P < 0.01$), 5.15 Gy/GBq (5 studies, 81 patients) and 4.35 Gy/GBq (1 study, 18 patients) for the submandibular glands ($P = 0.56$), 11.03 Gy/GBq (6 studies, 121 patients) and 19.23 Gy/GBq (3 studies, 53 patients) for the lacrimal glands ($P = 0.20$), 0.24 Gy/GBq (12 studies, 183 patients) and 0.19 Gy/GBq (4 studies, 68 patients) for the bone marrow ($P = 0.31$), and 1.11 Gy/GBq (9 studies, 154 patients) and 0.56 Gy/GBq (4 studies, 56 patients) for the liver ($P = 0.05$), respectively. Average tumor doses tended to be higher for [^{177}Lu]Lu-PSMA-617 than for [^{177}Lu]Lu-PSMA-I&T in soft tissue tumor lesions (4.19 vs. 2.94 Gy/GBq; $P = 0.26$). Dosimetry data of [^{177}Lu]Lu-J591 were limited to one published study of 35 patients with reported absorbed doses of 1.41, 0.32, and 2.10 Gy/GBq to the kidney, bone marrow, and liver, respectively. **Conclusion:** In this metaanalysis, there was no significant difference in absorbed dose between [^{177}Lu]Lu-PSMA-I&T and [^{177}Lu]Lu-PSMA-617. There was a possible trend toward a higher kidney dose with [^{177}Lu]Lu-PSMA-I&T and a higher tumor lesion dose with [^{177}Lu]Lu-PSMA-617. It remains unknown whether this finding has any clinical impact. The dosimetry methodologies were strikingly heterogeneous among studies, emphasizing the need for standardization.

Received Jan. 16, 2024; revision accepted Apr. 29, 2024.

For correspondence or reprints, contact Jeremie Calais (jcalais@mednet.ucla.edu).

*Contributed equally to this work.

Guest Editor: Rodney Hicks, University of Melbourne

Published online Jul. 3, 2024.

Key Words: ^{177}Lu; PSMA; dosimetry; theranostics; metaanalysis; prostate cancer

J Nucl Med 2024; 65:1264–1271
DOI: 10.2967/jnumed.124.267452

Novel theranostic approaches using radiopharmaceuticals have emerged for treating metastatic castration-resistant prostate cancer. Because of its overexpression by most prostate cancers, prostate-specific membrane antigen (PSMA) represents a valid molecular target for radionuclide imaging and therapy. The physical properties and commercial availability of ^{177}Lu make it one of the most used radionuclides for radioligand therapy. After the positive results of the VISION trial (*1*), [^{177}Lu]Lu-PSMA-617 therapy (Pluvicto; Novartis) was approved by the Food and Drug Administration, and this treatment is now included in the National Comprehensive Cancer Network guidelines and reimbursed by the Centers for Medicare and Medicaid Services for patients with metastatic castration-resistant prostate cancer progressing after chemotherapy. Randomized phase 3 trials testing [^{177}Lu]Lu-PSMA-617 at earlier disease stages have completed their enrollment (PSMAfore NCT04689828 for prechemotherapy metastatic castration-resistant prostate cancer patients, PSMAddition NCT04720157 for patients with metastatic hormone-sensitive prostate cancer). Another small-molecule radioligand, [^{177}Lu]Lu-PSMA-I&T, is being investigated in 2 randomized phase 3 trials (SPLASH NCT04647526 and ECLIPSE NCT05204927), which also completed enrollment. The radiolabeled monoclonal antibody [^{177}Lu]Lu-J591 is being investigated in an ongoing randomized phase 3 trial (PROSTACT NCT04876651).

^{177}Lu decays by β^- emission with a half-life of 6.7 d. The average energy of the β-particles is 134 keV (maximum of 498 keV), with an average travel path of 0.670 mm in soft tissue. The energies of the primary γ-emissions are 113 keV (6.6%) and 208 keV (11%) (*2*). The γ-ray emissions allow for imaging of the drug biodistribution over multiple days using planar scintigraphy or SPECT/CT. Estimations of the radiation dose deposition in normal organs at risk and tumor lesions are required for regulatory purposes and essential for risk determinations. Dosimetry also carries the potential to assist in individualized patient management, including optimization of drug administration (injected activity per cycle, number of cycles, time interval between cycles).

With the expected approval of various [^{177}Lu]Lu-PSMA–targeted compounds, the question of how their efficacy and safety

profiles compare arises. However, to our knowledge, no head-to-head dosimetry comparison of the different [^{177}Lu]Lu-PSMA–targeted compounds has been conducted. Moreover, the reported radiation dose estimates for [^{177}Lu]Lu-PSMA can vary considerably because multiple technical parameters and methods impact organ and tumor dose estimates, such as image reconstruction parameters, acquisition practices, segmentation methods, dose calculation models, lesion sizes, or use of partial-volume correction (*3*–*5*).

Because direct comparisons among different therapeutic radiopharmaceutical are not feasible, we conducted a systematic review and metaanalysis to summarize the dosimetry of [^{177}Lu]Lu-PSMA-617, [^{177}Lu]Lu-PSMA-I&T, and [^{177}Lu]Lu-J591 in articles published as of November 2023.

MATERIALS AND METHODS

The Preferred Reporting Items for Systematic Reviews and Meta-Analyses (PRISMA) 2020 guidelines were followed to conduct this study (*6*) (checklist provided in supplemental materials, available at http://jnm.snmjournals.org).

Article Search

We created a comprehensive list of all dosimetry studies involving [^{177}Lu]Lu-PSMA therapy for prostate cancer and performed a systematic review and metaanalysis. We conducted an article search using advanced settings in PubMed and Google Scholar as of November 2023 (Fig. 1). Within articles, referenced publications regarding the dosimetry of [^{177}Lu]Lu-PSMA were also added to the database if not initially found on either platform.

Data Inclusion

The dosimetry data were extracted from each article in Gy/GBq for the normal organs (kidney, parotid and submandibular glands, lacrimal glands, liver, and bone marrow) at risk and for tumor lesions, which were separated into bone and nonbone lesions (soft tissue; i.e., visceral, lung, liver, and lymph nodes). Biological effective dose was not included.

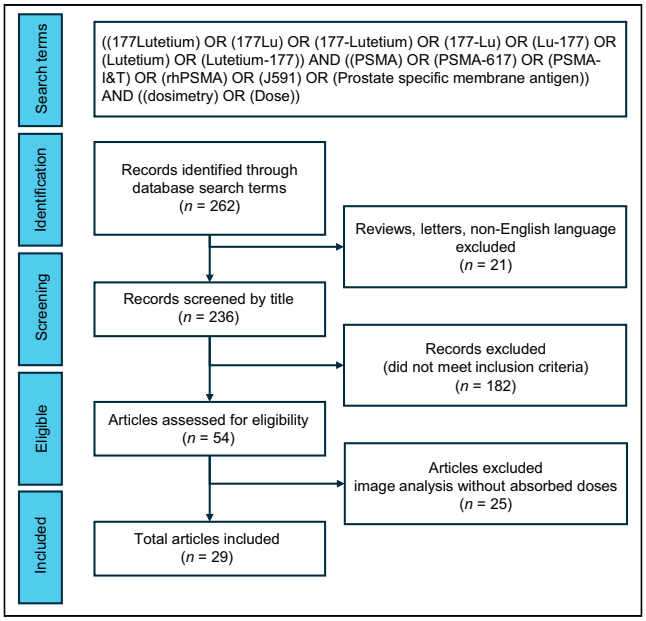

FIGURE 1. Study selection for metaanalysis. Using PRISMA criteria, we selected 29 studies for this metaanalysis. Only conference abstracts or fully published articles that were in English and reported absorbed dose to organs at risk or tumors were included.

Because of the different injected activities per cycle in each study, we also calculated the pooled dose normalized to a fixed amount of injected activity per cycle (Gy/cycle): 7.4 GBq for [^{177}Lu]Lu-PSMA-617 based on the VISION trial, 6.8 GBq for [^{177}Lu]Lu-PSMA-I&T based on the SPLASH trial, and 5.6 GBq (76 mCi ×2) for [^{177}Lu]Lu-J591 based on the PROSTACT trial.

Factors Affecting Dosimetry Calculations

We collected the multiple factors that could affect the dosimetry calculations. Three different image protocols were recorded: planar whole-body scans, 3-dimensional SPECT/CT scans, and a hybrid approach combining both. To convert activity to dose, multiple dosimetry tools were used, primarily including voxelwise and RADAR (Radiation Dose Assessment Resource; https://www.doseinfo-radar.com/) schema (OLINDA/EXM) or MIRD. In addition, different reconstruction parameters were used in the various studies. The 2 methods used to determine the average absorbed dose to bone marrow were based on blood sampling and on imaging.

Statistics

A metaanalysis was conducted for each organ (kidney, parotid and submandibular glands, lacrimal glands, bone marrow, and liver) and for tumor lesions. We reported the pooled estimated average dose of each radiopharmaceutical (617, I&T, and J591) with standard errors or CIs estimated using inverse variance weighting. Most studies reported their sample size, means, and SDs, which were used as inputs to the metaanalysis; however, some studies reported medians and quartiles instead. For those studies, we estimated the mean and SD by assuming the median was the mean and estimating the SD by taking the difference in quartiles divided by 1.35, as suggested by the *Cochrane Handbook for Systematic Reviews of Interventions* (*7*). The Cochran Q statistic and I^2 index (the percentage of variation across studies that is due to heterogeneity rather than chance) were used to assess heterogeneity. Because significant heterogeneity was observed, the random-effects metaanalytic model was used as opposed to the fixed-effects pooled estimate. Within each organ, we used the subgroup option of the package to test for differences in radionuclides. If the overall test was significant, we conducted pairwise comparisons between groups. However, if it was not significant, no further testing for that organ was done. Tumor dosimetry was analyzed for all lesions, as well as stratified by bone only or nonbone lesions. Statistical analyses were performed using R version 4.1.0 (www.r-project.org) with the meta package, which is the general package for metaanalysis. P values of less than 0.05 were considered statistically significant. The P values shown throughout the article denote comparisons between [^{177}Lu]Lu-PSMA-617 and [^{177}Lu]Lu-PSMA-I&T, as [^{177}Lu]Lu-J591 data were limited, unless otherwise indicated as overall P value.

RESULTS

Twenty-nine published articles comprising 535 patients were included in the metaanalysis. The number of studies and included patients for individual organs and tumor lesions are summarized in Supplemental Tables 1 and 2. The patient population is summarized in Supplemental Table 3. Overall, 90% of the studies in this metaanalysis included metastatic castration-resistant prostate cancer, whereas 10% included metastatic hormone-sensitive prostate cancer. Of note, one study included only low-volume metastatic hormone-sensitive prostate cancer (n = 10 patients) (*8,9*). The dosimetry protocol parameters and reconstruction protocols used in each study are included in Supplemental Tables 4 and 5.

The dosimetry data extracted from each article are summarized in Table 1 for the normal organs at risk and in Table 2 for the tumor lesions. Table 3 lists the average absorbed dose in Gy/GBq and the dose normalized to the injected activity (Gy). The pooled

TABLE 1
Reported Dosimetry for Organs at Risk

Author	Isotope	Injected activity (GBq)	Kidney (Gy/GBq)	Parotid (Gy/GBq)	Submandibular (Gy/GBq)	Marrow (Gy/GBq)	Liver (Gy/GBq)	Lacrimal (Gy/GBq)
Kabasakal (*39*)	617	0.2	0.88 ± 0.4	1.17 ± 0.31	–	0.03 ± 0.01	0.28 ± 0.09	–
Delker (*15*)	617	3.6	0.6 ± 0.18	1.4 ± 0.53	–	0.01 ± 0.01	0.11 ± 0.06	–
Fendler (*10*)	617	3.7	0.55 ± 0.25	1 ± 0.6	–	0.1	< 0.1	–
Hohberg (*40*)	617	5.5	0.53 ± 0.17	0.72 ± 0.14	–	–	–	2.82 ± 0.76
Kratochwil (*33*)	617	3.0	0.75 ± 0.19	1.28 ± 0.4	1.48 ± 0.37	0.03 ± 0.01	–	–
Yadav (*12*)	617	2.5	0.99 ± 0.31	1.24 ± 0.27	–	0.05 ± 0.06	0.36 ± 0.11	–
Scarpa (*19*)	617	6.1	0.6 ± 0.36	0.56 ± 0.25	0.5 ± 0.15	0.04 ± 0.03	–	1.01 ± 0.69
Gosewisch (*41*)	617	3.7	–	–	–	0.01 (0.01–0.02)	–	–
Gosewisch (*42*)	617	5.2	–	–	–	0.012	–	–
Sarnelli (*43*)	617	5.0	0.67 ± 0.27	0.81 ± 0.74	–	0.04 ± 0.02	0.16 ± 0.15	–
Violet (*20*)	617	7.8	0.39 ± 0.15	0.58 ± 0.43	0.44 ± 0.36	0.11 ± 0.1	0.1 ± 0.05	0.36 ± 0.18
Paganelli (*44*)	617	4.4	0.41 ± 0.19	1.04 ± 0.82	0.67 ± 0.36	0.04 ± 0.02	0.18 ± 0.14	2.06 ± 1.24
Mix (*34*)	617	6.0	0.67 ± 0.24	–	–	–	–	–
Privé/Peters (*8,9*)	617	3.0	0.49 ± 0.11	0.39 ± 0.17	–	0.02 ± 0.01	0.09 ± 0.01	–
Rosar (*11*)	617	6.4	0.54 ± 0.28	0.81 ± 0.34	0.72 ± 0.39	–	0.1 ± 0.05	–
Völter (*45*)	617	6.0	–	–	–	–	–	–
Kamaldeep (*16*)	617	4.4	0.49 ± 0.17	0.53 ± 0.2	–	0.03 ± 0.02	0.07 ± 0.04	1.23 ± 0.7
Schuchardt (*46*)	617	6.5	0.8	0.5	–	–	–	5.1
Herrmann/Krause (*47,48*)	617	7.4	0.43 ± 0.16	0.63 ± 0.36	–	0.04 ± 0.02	–	2.1 ± 0.47
Uijen (*22*)	617	3.0	0.49 (0.34–0.66)	–	–	–	–	–
Okamoto (*35*)	I&T	7.4	0.72 ± 0.21	0.55 ± 0.14	0.64 ± 0.4	–	0.12 ± 0.06	3.8 ± 1.4
Baum (*17*)	I&T	5.8	0.8 (0.2–1.9)	1.3 (0.3–9.5)	–	0.03 (0.01–0.04)	–	–
Barna (*13*)	I&T	7.4	0.71 ± 0.24	0.77	–	–	0.27	–
Chatachot (*14*)	I&T	6.7	0.81 ± 0.24	0.21 ± 0.14	–	0.02 ± 0.01	0.13 ± 0.10	3.62 ± 1.78
Schuchardt (*46*)	I&T	6.1	0.9	0.5	–	–	–	3.7
Kelk (*49*)	I&T	7.4	0.305	0.11	0.24	–	0.03	0.8
Feuerecker (*18*)	I&T	7.3	0.73 ± 0.18	0.8 ± 0.41	–	0.28 ± 0.2	0.07 ± 0.03	–
Beauregard (*50*)	I&T	6.8	0.73 ± 0.33	0.34 ± 0.27	–	0.03 ± 0.02	0.05 ± 0.04	1.2 ± 1.2
Uijen (*22*)	I&T	7.4	0.73 (0.42–1.31)	–	–	–	–	–
Resch (*51*)	I&T	7.4	2 (1.2–2.4)	–	–	–	–	–
Hohberg (*21*)	I&T	7.2	0.53 ± 0.21	–	–	–	–	–
Bander/Vallabhajosula (*27,52*)	J591	2.8	1.41 ± 0.35	–	–	0.32 ± 0.01	2.1 ± 0.6	–

Data are reported as mean ± SD or as median followed by range in parentheses.

TABLE 2
Reported Tumor Lesion Dosimetry

Author	Isotope	Injected activity (GBq)	Unspecified/single-study exploration (Gy/GBq)	Skeletal lesion (Gy/GBq)	Nodal lesion (Gy/GBq)	Liver lesion (Gy/GBq)
Delker (*15*)	617	3.6	2.1 ± 0.8*	5.3 ± 3.7	4.2 ± 5.3	–
Fendler (*10*)	617	3.7	2.16 ± 0.85*	4.92 ± 3.54	11.64 ± 5.44	–
Scarpa (*19*)	617	6.1	–	3.4 ± 1.9	2.6 ± 0.4	2.4 ± 0.8
Violet (*20*)	617	7.8	–	5.28 ± 2.46	3.91 ± 3.93	–
Paganelli (*44*)	617	4.4	–	4.7 (0.74–55.86)	3.64 (0.25–15.10)	–
Privé/Peters (*8,9*)	617	3.0	3.25 ± 3.19	1.1 (0.3–3.1)	3.1 (0.6–13)	–
Rosar (*11*)	617	6.4	–	1.68 ± 1.32	–	–
Volter (*45*)	617	6.0	–	4.7 ± 3.9	7.7 ± 9.7	–
Schuchardt (*46*)	617	6.5	–	6	7.1	–
Herrmann/Krause (*47,48*)	617	7.4	–	14.6 ± 29.8	12.5 ± 15.9	–
Okamoto (*35*)	I&T	7.4	1.75 ± 0.92†	3.4 ± 2.7	3.2 ± 2.2	1.2 ± 0.67
Baum (*17*)	I&T	5.8	–	3 (0.2–40)	4 (0.14–78)	–
Barna (*13*)	I&T	7.4	–	4.38	5.47	4.95
Schuchardt (*46*)	I&T	6.1	–	5.9	6.9	–
Feuerecker (*18*)	I&T	7.3	–	1.7 ± 1.13	4.51 ± 2.69	–
Hohberg (*21*)	I&T	7.2	–	3.47 ± 2	3.73 ± 1.65	–
Resch (*51*)	I&T	7.5	–	5.8 ± 3.1	7.7 ± 4.5	–

*Tumor was deemed soft tissue in nature.
†Tumor was deemed lung lesion.
Data are reported as mean ± SD or as median followed by range in parentheses.

averages and CIs are shown in Figures 2 and 3 for the kidney and tumors and in the supplemental materials for the other organs.

Kidneys

Twenty-eight studies including 485 patients reported kidney dosimetry. The absorbed kidney dose was not significantly different but tended to be higher for [^{177}Lu]Lu-PSMA-I&T than for [^{177}Lu]Lu-PSMA-617 (4.70 Gy [CI, 4.16–5.24 Gy] vs. 4.04 Gy [CI, 3.94–4.60 Gy]; $P = 0.10$). For [^{177}Lu]Lu-J591, the reported kidney dose was 3.95 Gy (CI, 3.62–4.27 Gy; overall $P = 0.06$) (Table 3). Figure 2 depicts the pooled average absorbed kidney dose along with the CI from the included studies.

Of note, Fendler et al. ([^{177}Lu]Lu-PSMA-617) reported the dose to the left and right kidneys individually, and we averaged the data

TABLE 3
Weighted Average of Absorbed Doses for Organs at Risk and Tumors

	617		I&T		J591			
Organ or group	Gy/GBq	Gy/7.4-GBq cycle	Gy/GBq	Gy/6.8-GBq cycle	Gy/GBq	Gy/5.6-GBq cycle	617 vs. I&T *P*	Overall *P*
Kidney	0.58	4.04	0.71	4.70	1.41	3.95	0.10	0.06
Parotid	0.84	5.85	0.43	2.62	–	–	<0.01	–
Submandibular	0.74	5.15	0.64	4.35	–	–	0.56	–
Bone marrow	0.03	0.24	0.03	0.19	0.32	0.90	0.31	<0.01
Liver	0.16	1.11	0.09	0.56	2.10	5.88	0.05	<0.01
Lacrimal glands	1.58	11.03	2.83	19.23	–	–	0.20	–
Tumor lesion, bone only	3.57	26.43	4.10	27.87	–	–	0.38	–
Tumor lesion, soft-tissue only	4.19	31.00	2.94	19.98	–	–	0.23	–

Data are summary of pooled doses for organs at risk and tumor lesions from different ^{177}Lu-based molecules shown as average (CI can be seen for kidney and tumors in Figs. 2 and 3 and for rest of organs in Supplemental Figs. 1–5).

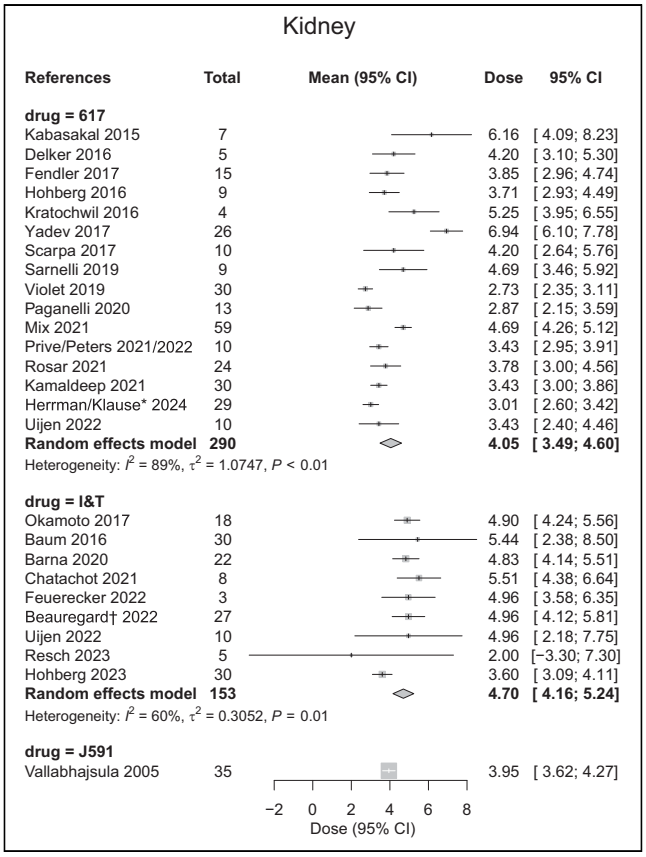

FIGURE 2. Reported absorbed doses (Gy/cycle) to kidney from selected studies, allowing for computation of pooled average absorbed dose. *As reported in VISION trial. †As reported in SPLASH trial.

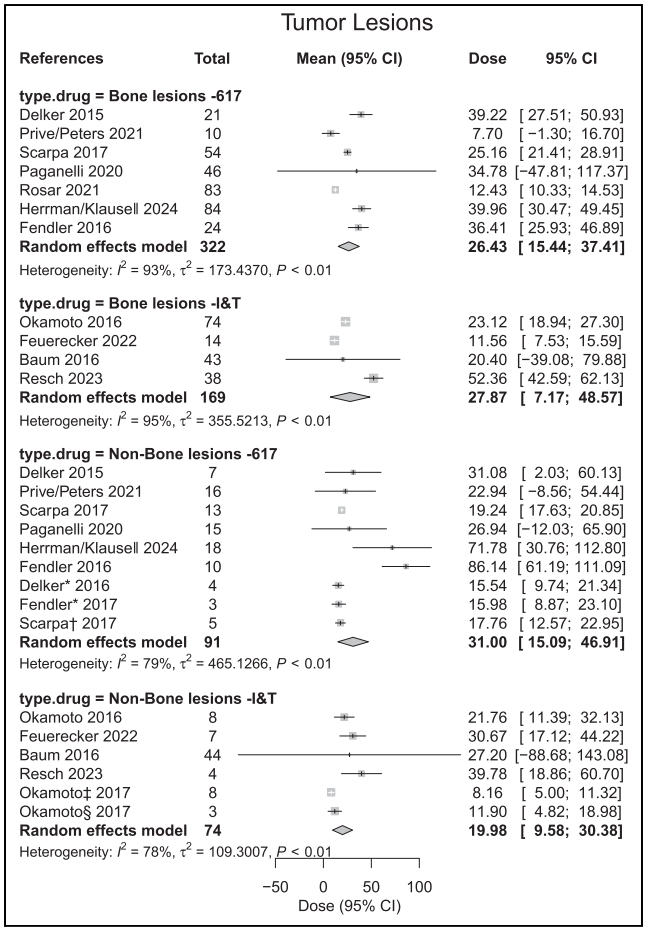

FIGURE 3. Reported absorbed doses (Gy/cycle) to tumor lesions from selected studies that were used to compute pooled average absorbed dose. Individual study estimates: gray box with black bar, each study's effect estimate (mean) is represented by gray box, with size of box proportional to study's weight in metaanalysis; black bar through box indicates CI for estimate; white cross in gray box, studies with very precise estimates; white cross indicates point estimate (mean), with gray box showing narrow CI; pooled estimate (diamond): Diamond Shape: The pooled estimate, or overall effect estimate, of the meta-analysis is shown as a diamond at the bottom of the plot. Width of the Diamond: The width of the diamond represents the confidence interval for the pooled estimate. The left and right tips of the diamond correspond to the lower and upper bounds of the CI, respectively. Center of the Diamond: The center of the diamond represents the overall effect estimate (mean) calculated from combining the individual study estimates. *Lesion location reported as soft tissue. †Lesion location reported as visceral tissue. ‡Lesion location reported within liver. §Lesion location reported within lung. ‖Tumor dosimetry reported from VISION trial.

to match other reports (*10*). Rosar et al. ([^{177}Lu]Lu-PSMA-617) reported dosimetry from multiple methods (*11*). We elected to include the values derived from the 3-dimensional SPECT images (highest reliability). Yadav et al. used a 2-L cocktail of lysine and arginine in saline to protect the kidneys 30–60 min before infusion, which may have affected dosimetry (*12*).

Liver

Fourteen studies reported liver dosimetry in 245 patients. The pooled liver doses are summarized in Table 3 and Supplemental Figure 1. The average absorbed dose to the liver was higher for [^{177}Lu]Lu-PSMA-617 than for [^{177}Lu]Lu-PSMA-I&T (1.11 Gy [CI, 0.65–1.58 Gy] vs. 0.56 Gy [0.28–0.84 Gy]; $P = 0.05$). The absorbed dose to the liver was highest for [^{177}Lu]Lu-PSMA-J591 (5.88 Gy [CI, 5.32–6.44 Gy]; overall $P < 0.01$). Two articles were excluded as the data were presented without SE or CIs (*10,13*).

Salivary Glands

Parotid and submandibular gland dosimetry was available from 20 and 7 studies that included 309 and 100 patients in total, respectively. The absorbed parotid gland dose was significantly higher for [^{177}Lu]Lu-PSMA-617, at 5.85 Gy (CI, 4.67–7.02 Gy), than for [^{177}Lu]Lu-PSMA-I&T, at 2.62 Gy (CI, 1.33–3.80 Gy) ($P < 0.01$). No significant difference was noted for the dose to the submandibular glands ($P = 0.56$) (Table 3; Supplemental Figs. 2 and 3). Absorbed dose values for the salivary glands have yet to be reported for [^{177}Lu]Lu-J591.

Applying ice packs locally to the neck to reduce blood flow did not affect the absorbed dose to the parotid glands (Table 1) (*10,14,15*).

Lacrimal Glands

Nine studies including 174 patients reported lacrimal gland dosimetry. The average absorbed dose to the lacrimal glands tended to be lower for [^{177}Lu]Lu-PSMA-617 than for [^{177}Lu]Lu-PSMA-I&T (11.03 Gy [CI, 6.00–16.06 Gy] vs. 19.23 Gy [CI, 7.69–30.78 Gy]; $P = 0.20$) (Table 3; Supplemental Fig. 4). Lacrimal gland dose has not been reported for [^{177}Lu]Lu-J591.

Bone Marrow

Eighteen studies including 293 patients reported bone marrow dosimetry. The absorbed doses reported were derived from blood sampling or SPECT/CT images ($n = 2$) for [^{177}Lu]Lu-PSMA-617 (*15,16*) and [^{177}Lu]Lu-PSMA-I&T (*14,17,18*). For [^{177}Lu]Lu-J591, the imaging method was used.

Absorbed dose values were similar for [^{177}Lu]Lu-PSMA-617 and [^{177}Lu]Lu-PSMA-I&T (0.24 Gy [CI, 0.17–0.31 Gy] vs. 0.19 Gy [CI, 0.13–0.25 Gy]; $P = 0.31$) but were significantly higher for [^{177}Lu]Lu-PSMA-J591 (0.90 Gy [CI, 0.89–0.91 Gy]; overall $P < 0.1$) (Table 3; Supplemental Fig. 5).

Tumor Lesion Dosimetry

In total, 339 patients and 656 lesions were reported from the studies seen in Table 2; 491 lesions from 161 patients were bone lesions, whereas 165 lesions from 178 patients were soft-tissue lesions. Although included in the absorbed dose analysis, the number or location of lesions present in the patient cohorts were not reported for several studies (*8,9,19–21*). The pooled average absorbed dose along with the CI from the included studies for the tumors can be seen in Table 3 and Figure 3.

Average tumor doses tended to be higher for [^{177}Lu]Lu-PSMA-617 than for [^{177}Lu]Lu-PSMA-I&T in soft tissue (31.00 Gy [CI, 15.09–46.91 Gy] vs. 19.98 Gy [CI, 9.58–30.38 Gy]; $P = 0.26$). [^{177}Lu]Lu-PSMA-617 and [^{177}Lu]Lu-PSMA-I&T achieved comparable bone lesion doses (26.43 Gy [CI, 15.44–37.41 Gy] vs. 27.78 Gy [CI, 7.17–48.57 Gy]; $P = 0.90$).

Impact of Image Acquisition Protocol on Reported Doses

Supplemental Table 4 denotes the imaging protocol, scanner, and activity-to-dose conversion method used in the study. We completed a simple comparison of the published absorbed doses between SPECT/CT, hybrid, and planar acquisition methods (Supplemental Figs. 6 and 7). Briefly, the difference between the average dose reported based on the imaging acquisition protocols was influenced primarily by the size of the organ (Supplemental Fig. 6). As the organ volume decreased, the reported absorbed dose decreased when serial SPECT imaging was used as opposed to the other methods. This trend continued when the tumor lesions were evaluated (Supplemental Fig. 7).

Although differences between scanners do not play a large role in the absorbed dose calculation, the reconstruction parameters have been shown to affect measurements (*5*). Although seldom reported, in Supplemental Table 5 we show the reconstruction parameters used. It is unknown to what extent these influenced the absorbed dose calculation.

DISCUSSION

In this systematic review and metaanalysis, we compared the organ and tumor dose estimates of 3 [^{177}Lu]Lu-PSMA–targeted radiopharmaceuticals provided by 29 studies that included 535 patients. All 3 [^{177}Lu]Lu-PSMA compounds had absorbed doses to organs at risk well below the regulatory threshold. Historically, the kidney is the dose-limiting organ for regulatory purposes, restricting the therapeutic injection of higher injected activities. For [^{177}Lu]Lu-PSMA-617 and [^{177}Lu]Lu-PSMA-I&T, however, the dose-limiting organs by regulatory threshold are the salivary and lacrimal glands (*22,23*). For [^{177}Lu]Lu-J591, in contrast, the liver and bone marrow are dose-limiting and the dosimetry of other organs has not been reported (*24,25*).

[^{177}Lu]Lu-PSMA-I&T and [^{177}Lu]Lu-PSMA-617 differed only in absorbed dose to the parotid glands ($P < 0.01$). There was no significant difference in absorbed dose between [^{177}Lu]Lu-PSMA-I&T and [^{177}Lu]Lu-PSMA-617 in the other organs or tumor lesions even if there was a possible trend toward a higher kidney dose with [^{177}Lu]Lu-PSMA-I&T (weighted average, 4.04 vs. 4.70 Gy; $P = 0.10$). The trend toward lower kidney doses from [^{177}Lu]Lu-PSMA-617 than from [^{177}Lu]Lu-PSMA-I&T may be explained by the neutrally charged chelator DOTA of [^{177}Lu]Lu-PSMA-617 compared with the negatively charged chelator DOTAGA of [^{177}Lu]Lu-PSMA-I&T (-1). This negatively charged chelator can increase reabsorption of the ligand by the proximal tubule of the kidney and thus may result in a higher absorbed kidney dose (*26*). [^{177}Lu]Lu-PSMA-617 and [^{177}Lu]Lu-PSMA-I&T showed similar binding characteristics in tumors.

Clinical studies investigating [^{177}Lu]Lu-J591 tumor doses have not been published. However, tumor uptake may be higher because of longer radiopharmaceutical retention as shown in preclinical models (*27*).

Dosimetry protocols and technical parameters varied substantially among studies (image acquisition parameters, image reconstruction parameters, quantification methods, dose calculation methodologies, bone marrow dosimetry, first cycle vs. multiple cycles, etc.). Three-dimensional SPECT/CT, planar imaging, or a combination of the two (hybrid) can be performed on patients injected with [^{177}Lu]Lu-PSMA compounds. Multiple-time-point 3-dimensional SPECT/CT is viewed as the most accurate imaging technique to perform these calculations. We performed a simple comparison of the imaging techniques from the various published articles to the effect on the dosimetry and support the findings of Rosar et al. (*9*). Using planar-only imaging in dosimetry calculations results in higher uncertainty than using hybrid or SPECT/CT protocols (*5,11*). A detailed analysis of the impact of acquisition and reconstruction parameters on the derived doses was not feasible because of the limited information in the respective publications (Supplemental Tables 4 and 5). Most of the authors used the OLINDA/EXM software (based on MIRDDOSE 3.0/3.1 (*28*)) in their calculations of absorbed dose (https://www.doseinfo-radar.com/RADAROver.html). The difference between OLINDA/EXM and voxel-based techniques is the use of dose point kernels with patient-specific geometries of both organs and tumors in the latter, whereas OLINDA/EXM relies on phantom data.

Organ dosimetry of all 3 compounds was well within regulatory limits. It is worth mentioning that dose thresholds applied by regulatory agencies are likely inappropriate for RPT as there has been no formal dose–toxicity analysis. The current thresholds are derived from one work done in 1991 using conventional fractionated external-beam radiation therapy (*29*). Some authors correct the data presented from external-beam radiation therapy for RPT, suggesting that the absorbed kidney dose limit is closer to 39 Gy (expanded further in the supplemental materials) (*30–32*). Only a few studies have reported whether the number of RPT cycles (*14–16,33–35*) has an impact on kidney doses (*36,37*) or whether the injected activity has an impact on outcomes (*38*). There is a need to provide new thresholds specific to RPT along with developing proven radioprotection methods (prior methods are given in the supplemental materials). Monitoring of the short-term and long-term toxicity of RPT, and the correlation of observed clinical toxicity with dosimetry, is further warranted. Efforts to obtain a new expert consensus on these topics, such as the RPT-TEC group, should be encouraged and promoted.

This study had some limitations. The included studies were heterogeneous in terms of patient population and treatment protocols. Although seldom noted, the reconstruction parameters used were vastly different, which has been shown to have a profound effect on absorbed dose calculations. Partial-volume effect corrections were not mentioned in any of the published articles. The lack of standardization in imaging and dosimetry is the major obstacle in comparing results from many studies and pooling data.

CONCLUSION

In this metaanalysis, we provided doses estimates of [^{177}Lu]Lu-PSMA radiopharmaceuticals from 29 studies and 535 patients. There was no significant difference in absorbed dose between [^{177}Lu]Lu-PSMA-I&T and [^{177}Lu]Lu-PSMA-617 even if there was a possible trend toward a higher kidney dose with [^{177}Lu]Lu-PSMA-I&T and toward a higher tumor lesion dose with [^{177}Lu]Lu-PSMA-617. It remains unknown whether the higher tumor-to-kidney dose for PSMA-617 has any relevant impact on clinical outcomes such as progression-free or overall survival. The dosimetry methodologies were strikingly heterogeneous among studies, emphasizing the need for standardization.

DISCLOSURE

Jeremie Calais reports grants from support to his institution from Lantheus, Novartis, and POINT Biopharma. He also reports consulting activities (advisory board member, speaker, blinded reader) for Advanced Accelerator Applications, Amgen, Astellas, Bayer, Blue Earth Diagnostics Inc., Curium Pharma, DS Pharma, Fibrogen, GE Healthcare, Isoray, IBA RadioPharma, Janssen Pharmaceuticals, Monrol, Lightpoint Medical, Lantheus, Novartis, Pfizer, POINT Biopharma, Progenics, Radiomedix, Sanofi, Siemens-Varian, SOFIE, and Telix Pharmaceuticals, outside the submitted work. Statistical analyses for this research were supported by the National Center for Advancing Translational Science (NCATS) of the National Institutes of Health under UCLA Clinical and Translational Science Institute grant UL1TR001881. No other potential conflict of interest relevant to this article was reported.

KEY POINTS

QUESTION: Are there any differences among the dosimetry of [^{177}Lu]Lu-PSMA-617, [^{177}Lu]Lu-PSMA-I&T, and [^{177}Lu]Lu-J591?

PERTINENT FINDINGS: In this metaanalysis, we provided doses estimates of [^{177}Lu]Lu-PSMA radiopharmaceuticals from 29 studies and 535 patients. There was no significant difference in absorbed dose between [^{177}Lu]Lu-PSMA-I&T and [^{177}Lu]Lu-PSMA-617, although there was a possible trend toward a higher kidney dose with [^{177}Lu]Lu-PSMA-I&T and toward a higher tumor lesion dose with [^{177}Lu]Lu-PSMA-617. The lack of standardization in imaging and dosimetry is a major obstacle in comparing results from many studies and pooling data.

IMPLICATIONS FOR PATIENT CARE: [^{177}Lu]Lu-PSMA-617, [^{177}Lu]Lu-PSMA-I&T, and [^{177}Lu]Lu-J591 absorbed doses were all below regulatory thresholds for all organs. Although [^{177}Lu]Lu-PSMA-I&T seems to have a lower tumor dose and higher kidney dose than those of [^{177}Lu]Lu-PSMA-617, the clinical relevance of this finding remains unknown. Standardized dosimetry practices are warranted for further clinical implementation.

REFERENCES

1. Sartor O, de Bono J, Chi KN, et al. Lutetium-177-PSMA-617 for metastatic castration-resistant prostate cancer. *N Engl J Med.* 2021;385:1091–1103.
2. Dash A, Pillai MR, Knapp FF Jr. Production of ^{177}Lu for targeted radionuclide therapy: available options. *Nucl Med Mol Imaging.* 2015;49:85–107.
3. Jackson PA, Hofman MS, Hicks RJ, Scalzo M, Violet J. Radiation dosimetry in ^{177}Lu-PSMA-617 therapy using a single posttreatment SPECT/CT scan: a novel methodology to generate time- and tissue-specific dose factors. *J Nucl Med.* 2020; 61:1030–1036.
4. Mora-Ramirez E, Santoro L, Cassol E, et al. Comparison of commercial dosimetric software platforms in patients treated with ^{177}Lu-DOTATATE for peptide receptor radionuclide therapy. *Med Phys.* 2020;47:4602–4615.
5. Tran-Gia J, Denis-Bacelar AM, Ferreira KM, et al. A multicentre and multi-national evaluation of the accuracy of quantitative Lu-177 SPECT/CT imaging performed within the MRTDosimetry project. *EJNMMI Phys.* 2021;8:55.
6. Page MJ, McKenzie JE, Bossuyt PM, et al. The PRISMA 2020 statement: an updated guideline for reporting systematic reviews. *Rev Esp Cardiol (Engl Ed).* 2021;74:790–799.
7. Higgens JPT, Green S, eds. *Cochrane Handbook for Systematic Reviews of Interventions.* Wiley Blackwell; 2008:section 7.7.3.5.
8. Peters SMB, Privé BM, de Bakker M, et al. Intra-therapeutic dosimetry of [^{177}Lu]Lu-PSMA-617 in low-volume hormone-sensitive metastatic prostate cancer patients and correlation with treatment outcome. *Eur J Nucl Med Mol Imaging.* 2022;49:460–469.
9. Privé BM, Peters SMB, Muselaers CHJ, et al. Lutetium-177-PSMA-617 in low-volume hormone-sensitive metastatic prostate cancer: a prospective pilot study. *Clin Cancer Res.* 2021;27:3595–3601.
10. Fendler WP, Reinhardt S, Ilhan H, et al. Preliminary experience with dosimetry, response and patient reported outcome after ^{177}Lu-PSMA-617 therapy for metastatic castration-resistant prostate cancer. *Oncotarget.* 2017;8:3581–3590.
11. Rosar F, Schon N, Bohnenberger H, et al. Comparison of different methods for post-therapeutic dosimetry in [^{177}Lu]Lu-PSMA-617 radioligand therapy. *EJNMMI Phys.* 2021;8:40.
12. Yadav MP, Ballal S, Tripathi M, et al. Post-therapeutic dosimetry of ^{177}Lu-DKFZ-PSMA-617 in the treatment of patients with metastatic castration-resistant prostate cancer. *Nucl Med Commun.* 2017;38:91–98.
13. Barna S, Haug AR, Hartenbach M, et al. Dose calculations and dose-effect relationships in ^{177}Lu-PSMA I&T radionuclide therapy for metastatic castration-resistant prostate cancer. *Clin Nucl Med.* 2020;45:661–667.
14. Chatachot K, Shiratori S, Chaiwatanarat T, Khamwan K. Patient dosimetry of ^{177}Lu-PSMA I&T in metastatic prostate cancer treatment: the experience in Thailand. *Ann Nucl Med.* 2021;35:1193–1202.
15. Delker A, Fendler WP, Kratochwil C, et al. Dosimetry for ^{177}Lu-DKFZ-PSMA-617: a new radiopharmaceutical for the treatment of metastatic prostate cancer. *Eur J Nucl Med Mol Imaging.* 2016;43:42–51.
16. Kamaldeep, Wanage G, Sahu SK, et al. Examining absorbed doses of indigenously developed ^{177}Lu-PSMA-617 in metastatic castration-resistant prostate cancer patients at baseline and during course of peptide receptor radioligand therapy. *Cancer Biother Radiopharm.* 2021;36:292–304.
17. Baum RP, Kulkarni HR, Schuchardt C, et al. ^{177}Lu-labeled prostate-specific membrane antigen radioligand therapy of metastatic castration-resistant prostate cancer: safety and efficacy. *J Nucl Med.* 2016;57:1006–1013.
18. Feuerecker B, Chantadisai M, Allmann A, et al. Pretherapeutic comparative dosimetry of ^{177}Lu-rhPSMA-7.3 and ^{177}Lu-PSMA I&T in patients with metastatic castration-resistant prostate cancer. *J Nucl Med.* 2022;63:833–839.
19. Scarpa L, Buxbaum S, Kendler D, et al. The ^{68}Ga/^{177}Lu theragnostic concept in PSMA targeting of castration-resistant prostate cancer: correlation of SUV_{max} values and absorbed dose estimates. *Eur J Nucl Med Mol Imaging.* 2017;44: 788–800.
20. Violet J, Jackson P, Ferdinandus J, et al. Dosimetry of ^{177}Lu-PSMA-617 in metastatic castration-resistant prostate cancer: correlations between pretherapeutic imaging and whole-body tumor dosimetry with treatment outcomes. *J Nucl Med.* 2019;60:517–523.
21. Hohberg M, Reifegerst M, Drzezga A, Wild M, Schmidt M. Prediction of response to $_{177}$Lu-PSMA therapy based on tumor-to-kidney ratio on pretherapeutic PSMA PET/CT and posttherapeutic tumor-dose evaluation in mCRPC. *J Nucl Med.* 2023;64:1758–1764.
22. Uijen MJM, Prive BM, van Herpen CML, et al. Kidney absorbed radiation doses for [^{177}Lu]Lu-PSMA-617 and [^{177}Lu]Lu-PSMA-I&T determined by 3D clinical dosimetry. *Nucl Med Commun.* 2023;44:270–275.
23. Mahajan S, Grewal RK, Friedman KP, Schoder H, Pandit-Taskar N. Assessment of salivary gland function after ^{177}Lu-PSMA radioligand therapy: current concepts in imaging and management. *Transl Oncol.* 2022;21:101445.

24. Tagawa ST, Milowsky MI, Morris M, et al. Phase II study of lutetium-177-labeled anti-prostate-specific membrane antigen monoclonal antibody J591 for metastatic castration-resistant prostate cancer. *Clin Cancer Res.* 2013;19:5182–5191.
25. Hartrampf PE, Weinzierl FX, Buck AK, et al. Matched-pair analysis of [^{177}Lu]Lu-PSMA I&T and [^{177}Lu]Lu-PSMA-617 in patients with metastatic castration-resistant prostate cancer. *Eur J Nucl Med Mol Imaging.* 2022;49:3269–3276.
26. Vegt E, de Jong M, Wetzels JF, et al. Renal toxicity of radiolabeled peptides and antibody fragments: mechanisms, impact on radionuclide therapy, and strategies for prevention. *J Nucl Med.* 2010;51:1049–1058.
27. Bander NH, Milowsky MI, Nanus DM, Kostakoglu L, Vallabhajosula S, Goldsmith SJ. Phase I trial of ^{177}lutetium-labeled J591, a monoclonal antibody to prostate-specific membrane antigen, in patients with androgen-independent prostate cancer. *J Clin Oncol.* 2005;23:4591–4601.
28. Stabin MG, Sparks RB, Crowe E. OLINDA/EXM: the second-generation personal computer software for internal dose assessment in nuclear medicine. *J Nucl Med.* 2005;46:1023–1027.
29. Emami B, Lyman J, Brown A, et al. Tolerance of normal tissue to therapeutic irradiation. *Int J Radiat Oncol Biol Phys.* 1991;21:109–122.
30. Zechmann CM, Afshar-Oromieh A, Armor T, et al. Radiation dosimetry and first therapy results with a ^{124}I/^{131}I-labeled small molecule (MIP-1095) targeting PSMA for prostate cancer therapy. *Eur J Nucl Med Mol Imaging.* 2014;41:1280–1292.
31. Bodei L, Cremonesi M, Grana CM, et al. Peptide receptor radionuclide therapy with ^{177}Lu-DOTATATE: the IEO phase I-II study. *Eur J Nucl Med Mol Imaging.* 2011;38:2125–2135.
32. Sandström M, Freedman N, Fross-Baron K, Kahn T, Sundin A. Kidney dosimetry in 777 patients during ^{177}Lu-DOTATATE therapy: aspects on extrapolations and measurement time points. *EJNMMI Phys.* 2020;7:73.
33. Kratochwil C, Giesel FL, Stefanova M, et al. PSMA-targeted radionuclide therapy of metastatic castration-resistant prostate cancer with ^{177}Lu-labeled PSMA-617. *J Nucl Med.* 2016;57:1170–1176.
34. Mix M, Renaud T, Kind F, et al. Kidney doses in ^{177}Lu-based radioligand therapy in prostate cancer: is dose estimation based on reduced dosimetry measurements feasible? *J Nucl Med.* 2022;63:253–258.
35. Okamoto S, Thieme A, Allmann J, et al. Radiation dosimetry for ^{177}Lu-PSMA I&T in metastatic castration-resistant prostate cancer: absorbed dose in normal organs and tumor lesions. *J Nucl Med.* 2017;58:445–450.
36. Garin E, Tselikas L, Guiu B, et al. Personalised versus standard dosimetry approach of selective internal radiation therapy in patients with locally advanced hepatocellular carcinoma (DOSISPHERE-01): a randomised, multicentre, open-label phase 2 trial. *Lancet Gastroenterol Hepatol.* 2021;6:17–29.
37. Minczeles NS, de Herder WW, Feelders RA, Verburg FA, Hofland J, Brabander T. Long-term outcomes of submaximal activities of peptide receptor radionuclide therapy with ^{177}Lu-DOTATATE in neuroendocrine tumor patients. *J Nucl Med.* 2023;64:40–46.
38. Sundlöv A, Gleisner KS, Tennvall J, et al. Phase II trial demonstrates the efficacy and safety of individualized, dosimetry-based ^{177}Lu-DOTATATE treatment of NET patients. *Eur J Nucl Med Mol Imaging.* 2022;49:3830–3840.
39. Kabasakal L, AbuQbeitah M, Aygun A, et al. Pre-therapeutic dosimetry of normal organs and tissues of ^{177}Lu-PSMA-617 prostate-specific membrane antigen (PSMA) inhibitor in patients with castration-resistant prostate cancer. *Eur J Nucl Med Mol Imaging.* 2015;42:1976–1983.
40. Hohberg M, Eschner W, Schmidt M, et al. Lacrimal glands may represent organs at risk for radionuclide therapy of prostate cancer with [^{177}Lu]DKFZ-PSMA-617. *Mol Imaging Biol.* 2016;18:437–445.
41. Gosewisch A, Delker A, Tattenberg S, et al. Patient-specific image-based bone marrow dosimetry in Lu-177-[DOTA^0,Tyr^3]-octreotate and Lu-177-DKFZ-PSMA-617 therapy: investigation of a new hybrid image approach. *EJNMMI Res.* 2018;8:76.
42. Gosewisch A, Ilhan H, Tattenberg S, et al. 3D Monte Carlo bone marrow dosimetry for Lu-177-PSMA therapy with guidance of non-invasive 3D localization of active bone marrow via Tc-99m-anti-granulocyte antibody SPECT/CT. *EJNMMI Res.* 2019;9:76.
43. Sarnelli A, Belli ML, Di Iorio V, et al. Dosimetry of ^{177}Lu-PSMA-617 after mannitol infusion and glutamate tablet administration: preliminary results of EUDRACT/RSO 2016-002732-32 IRST protocol. *Molecules.* 2019;24:621.
44. Paganelli G, Sarnelli A, Severi S, et al. Dosimetry and safety of ^{177}Lu PSMA-617 along with polyglutamate parotid gland protector: preliminary results in metastatic castration-resistant prostate cancer patients. *Eur J Nucl Med Mol Imaging.* 2020; 47:3008–3017.
45. Völter F, Mittlmeier L, Gosewisch A, et al. Correlation of an index-lesion-based SPECT dosimetry method with mean tumor dose and clinical outcome after ^{177}Lu-PSMA-617 radioligand therapy. *Diagnostics (Basel).* 2021;11:428.
46. Schuchardt C, Zhang J, Kulkarni HR, Chen X, Muller D, Baum RP. Prostate-specific membrane antigen radioligand therapy using ^{177}Lu-PSMA I&T and ^{177}Lu-PSMA-617 in patients with metastatic castration-resistant prostate cancer: comparison of safety, biodistribution, and dosimetry. *J Nucl Med.* 2022;63:1199–1207.
47. Herrmann K, Rahbar K, Eiber M, et al. Renal and multiorgan safety of ^{177}Lu-PSMA-617 in patients with metastatic castration-resistant prostate cancer in the VISION dosimetry substudy. *J Nucl Med.* 2024;65:71–78.
48. Krause BJ, Chi KN, Sartor AO, et al. Tumor dosimetry of [^{177}Lu]Lu-PSMA-617 for the treatment of metastatic castration-resistant prostate cancer: results from the VISION trial sub-study [abstract]. *J Clin Oncol.* 2023;41:5046.
49. Kelk E, Ruuge P, Rohtla K, Poksi A, Kairemo K. Radiomics analysis for ^{177}Lu-DOTAGA-(l-y)fk(Sub-KuE) targeted radioligand therapy dosimetry in metastatic prostate cancer: a model based on clinical example. *Life (Basel).* 2021;11:170.
50. Beauregard J-M. Dosimetry results from the SPLASH trial. Paper presented at: 2022 Virtual SNMMI Mid-Winter and ACNM Annual Meeting; February 25–27, 2022.
51. Resch S, Takayama Fouladgar S, Zacherl M, et al. Investigation of image-based lesion and kidney dosimetry protocols for ^{177}Lu-PSMA-I&T therapy with and without a late SPECT/CT acquisition. *EJNMMI Phys.* 2023;10:11.
52. Vallabhajosula S, Goldsmith SJ, Hamacher KA, et al. Prediction of myelotoxicity based on bone marrow radiation-absorbed dose: radioimmunotherapy studies using ^{90}Y- and ^{177}Lu-labeled J591 antibodies specific for prostate-specific membrane antigen. *J Nucl Med.* 2005;46:850–858.